



REVIEW

Rheology of Paste in Mine Backfilling: Mechanisms, Models, and Key Influencing Factors

Mingzhi Zhang¹, Qian Zhang², Haonan Zhang², Xuecheng Shang³, Xionghuan Tan², Zheyuan Jiang⁴, Yun Lin¹, Junwei Shu², Tianxing Ma^{2,5,*} and Liangxu Shen^{2,*} 

¹School of Resources and Safety Engineering, Central South University, Changsha, China

²Ocean College, Zhejiang University, Zhoushan, China

³School of Transportation Engineering, Shandong Jianzhu University, Jinan, China

⁴Jiangsu Key Laboratory of Low Carbon and Sustainable Geotechnical Engineering, Institute of Geotechnical Engineering, Southeast University, Nanjing, China

⁵Department of Civil and Environmental Engineering, Hong Kong Polytechnic University, Hong Kong, China

*Corresponding Authors: Tianxing Ma. Email: m16673133031@163.com; Liangxu Shen. Email: shenliangxu@126.com

Received: 25 December 2025; Accepted: 06 March 2026; Published: 31 March 2026

ABSTRACT: The rheological behavior of paste in mine backfilling systems is governed by multiple coupled mechanisms, including particulate structure evolution, time-dependent effects, spatially heterogeneous flow, and scale dependence. As a result, its macroscopic response cannot be adequately described by a single material parameter or purely local constitutive relations. Although significant progress has been made in experimental characterization and empirical modeling, rheological parameters reported under different conditions remain difficult to reconcile, highlighting the limitations of existing models in capturing structural evolution and nonlocal effects. This review provides a concise synthesis of current advances in paste rheology for mine backfilling applications, with emphasis on yield behavior, shear-rate-dependent nonlinear flow response, thixotropy, and shear history effects. The applicability and limitations of commonly used rheological models, including the Bingham and Herschel–Bulkley models, are critically examined. Key factors influencing paste rheology—such as particle gradation, temperature, and chemical additives—are discussed from a structure-controlled perspective. Finally, physics-constrained data-driven approaches are highlighted as a promising direction for improving the description and prediction of complex rheological behavior. Overall, this review emphasizes the need to balance experimental observability, model simplicity, and physical consistency, and highlights the importance of linking microstructural mechanisms, scale effects, and macroscopic rheological response to establish more unified and engineering-relevant frameworks for paste rheology in mine backfilling systems.

KEYWORDS: Cemented paste backfill; rheological behavior; paste rheology; rheological modeling; yield behavior

1 Introduction

The continuous exploitation of mineral resources has imposed increasingly stringent requirements on underground stope management, tailings disposal, and environmental risk control [1–3]. Against this background, cemented paste backfill (CPB) has become an important technical approach for achieving safe and sustainable mining in mines, owing to its comprehensive advantages in tailings reutilization, underground stability control, and environmental risk reduction [4–8]. The engineering performance of paste backfill systems largely depends on the flow and deformation behavior of paste slurry during its

preparation, transportation, and placement processes [4,6]. Consequently, paste rheology has emerged as one of the key scientific and engineering issues constraining the practical application and optimization of paste backfill technology [9,10].

Although paste backfill technology has been widely applied in engineering practice, a unified understanding of the physical nature of the rheological behavior of high-concentration paste is still lacking [6,11,12]. Existing studies generally indicate that paste is a structure-sensitive particulate–fluid composite system, whose flow behavior exhibits pronounced nonlinearity, time dependence, and path dependence [11–14]. However, rheological parameters obtained under different experimental conditions, testing methods, and material systems often show substantial discrepancies [15–17], which limits the comparability of experimental results and the general applicability of engineering models [12,16]. Such inconsistencies, to some extent, reflect the insufficient understanding of microstructural evolution processes and spatial interaction effects within paste systems in existing theoretical frameworks [11,18].

From a modeling perspective, although empirical and semi-empirical rheological models are widely used in engineering calculations due to their practical value [6,19], most of these models are based on local constitutive assumptions and therefore struggle to describe the spatially heterogeneous flow behaviors commonly observed in paste systems [20–22]. In recent years, nonlocal rheology, structural parameter evolution models, and multiscale modeling approaches have been proposed in an attempt to overcome the limitations of conventional models [23–25]. Nevertheless, these models still face challenges in terms of physical interpretability, parameter identification, and general applicability across different paste systems [26], and a unified and experimentally verifiable theoretical framework has yet to be established. This indicates that research on paste rheology is currently at a critical stage of transition from empirical descriptions toward physically constrained modeling.

Over the past two decades, research on paste rheology has shown a clear temporal evolution in the English-language literature, as reflected in the publication trend summarized in Fig. 1. Early studies were relatively sparse, whereas publication activity has increased markedly since 2017, indicating growing academic and engineering interest in paste-based backfilling systems. Recent work has shifted from single-factor rheological characterization toward multi-factor coupling, time-dependent structural evolution, sustainable binders and additives, and data-assisted optimization. This transition motivates the integrated, mechanism-oriented perspective adopted in this review, as discussed below.

Against this background, recent advances in machine-learning approaches incorporating rheological physical constraints have emerged as a promising direction for addressing the complex behavior of paste in CPB systems [27–29]. These methods offer the potential to bridge empirical parameter prediction and mechanistic understanding, providing a more integrated framework for modeling paste rheology [30–33]. However, existing studies remain largely exploratory, and critical challenges persist regarding applicability, reliability, and integration with conventional rheological theories [34–37]. Unlike previous reviews that primarily emphasize empirical constitutive descriptions or isolated influencing factors, this review provides a critical synthesis of experimental observations, theoretical models, and emerging data-driven approaches from a structure-controlled perspective [38–41]. Particular attention is given to the roles of nonlocal effects and scale dependence in governing yield behavior, nonlinear flow response, and model applicability. Recent studies further indicate that integrating directly measurable operational variables and adopting robust learning and optimization strategies can enhance prediction stability and transferability under variable conditions [42–45]. To clarify the scope and logical structure of this review, a conceptual framework summarizing the rheology of paste in mine backfilling systems is presented in Fig. 2.

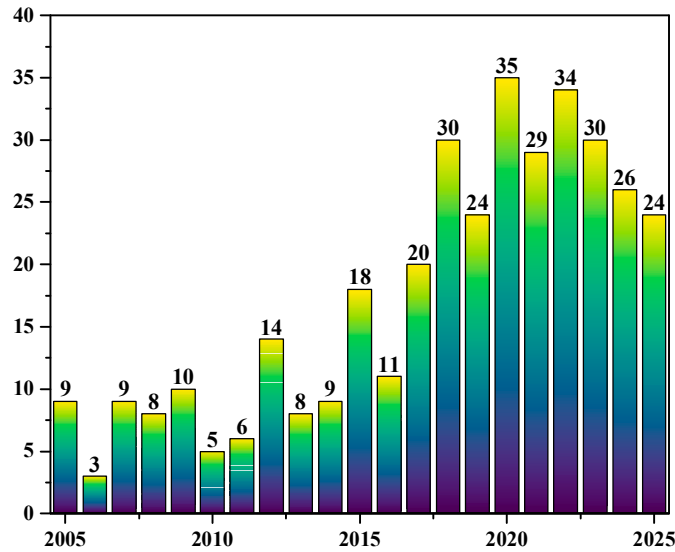


Figure 1: Annual Publication Trend of Studies on Paste backfilling Rheology (2005–2025).

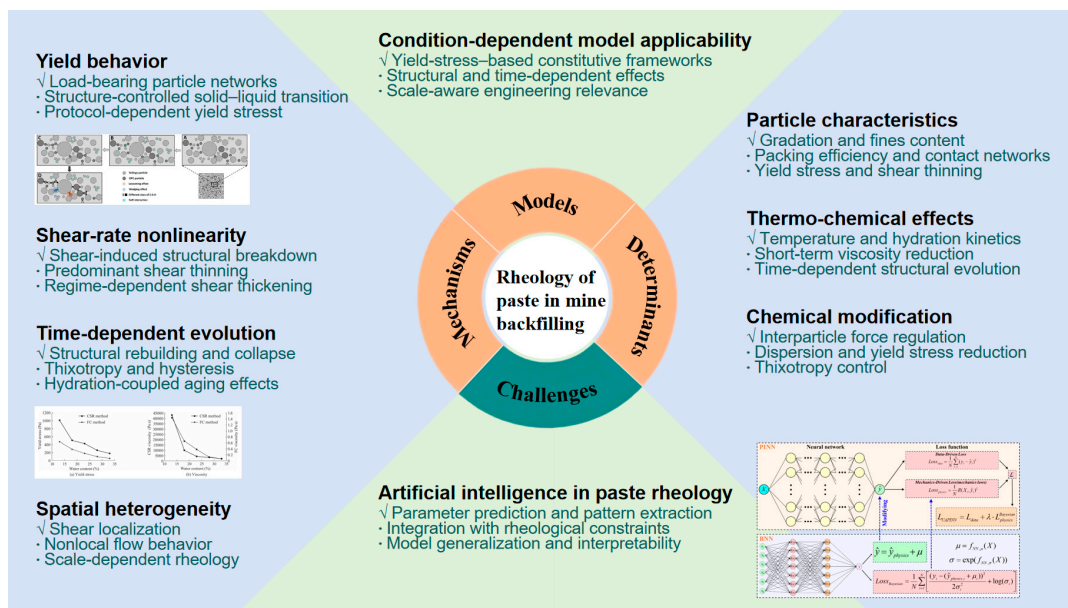


Figure 2: Conceptual framework summarizing the rheology of paste in mine backfilling.

2 Paste Rheological Properties

Paste is a high-concentration particulate–fluid composite, where macroscopic flow behavior is predominantly determined by the interactions between solid particles and the internal structural organization. Ideal paste backfill materials should contain at least 15% of particles smaller than 20 μm , along with sufficient water content [46,47]. Existing studies suggest that a saturation degree between 101.5% and 105.3% and a bleed water rate ranging from 1.5% to 5% can serve as additional performance indicators for paste materials [48]. Owing to the high solid volume fraction, such systems typically exhibit mechanical responses intermediate between those of solids and fluids, and are distinctly different from dilute suspensions or conventional non-Newtonian fluids. Under applied shear, paste systems may exhibit

characteristic rheological features such as yield behavior, nonlinear flow response, and time-dependent effects. These macroscopic manifestations reflect the dynamic adjustment of internal particulate structures in response to changes in loading conditions, and represent common rheological features of dense particulate systems. Fig. 3 schematically summarizes typical experimental frameworks reported in the literature for rheological characterization of CPB, including the rheological testing apparatus, the standardized testing procedure, and representative shear stress–shear rate responses of paste slurries.

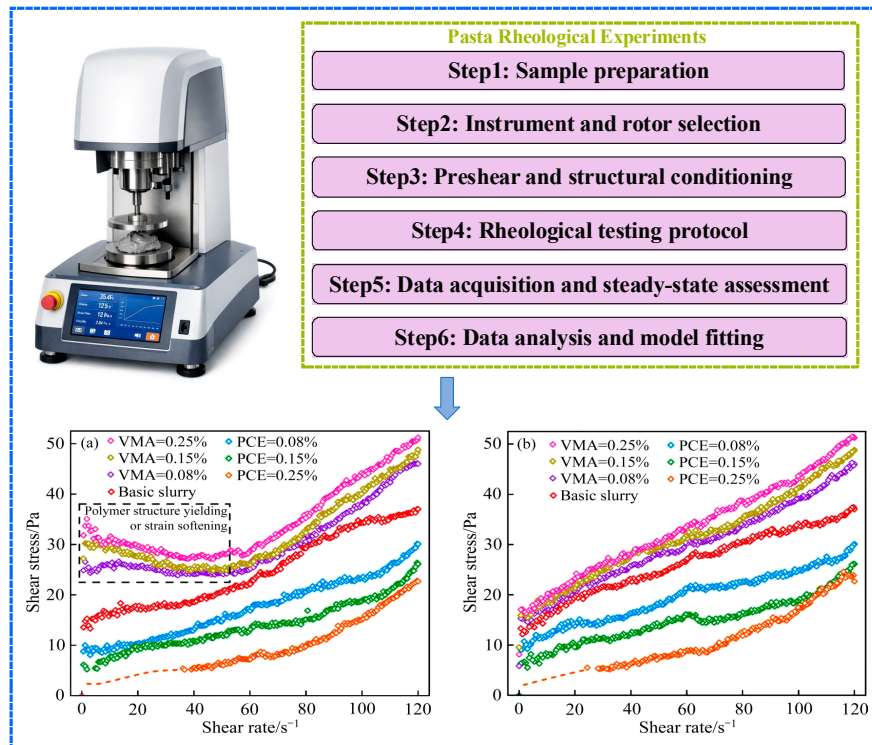


Figure 3: Schematic representation of the rheological testing framework for CPB and typical rheological curves of slurry under different admixture addition conditions: (a) Shear rate ascent stage; (b) Shear rate descent stage (adapted from Ref. [2]).

2.1 Yield Behavior and Structure-Controlled Solid–Liquid Transition

Yield behavior describes the mechanical response whereby a paste system exhibits solid-like characteristics when the applied shear stress remains below a critical value, undergoing only limited elastic or viscoelastic deformation. Once the applied stress exceeds this critical threshold, the internal load-bearing structure becomes unstable and collapses, leading to the onset of macroscopic flow [49]. This critical stress is commonly referred to as the yield stress, which distinguishes the solid-like and fluid-like states of paste systems [50]. As the applied shear stress approaches the yield stress, a pronounced change in shear rate is commonly observed, with the solid–fluid transition occurring at a finite shear rate, as schematically illustrated in Fig. 4 (adapted from Ref. [12]) based on representative observations reported in the literature. It should be noted that the sharpness of the transition and the associated shear rate at yielding may vary across studies, reflecting differences in particle size distribution, solid fraction, and testing geometry.

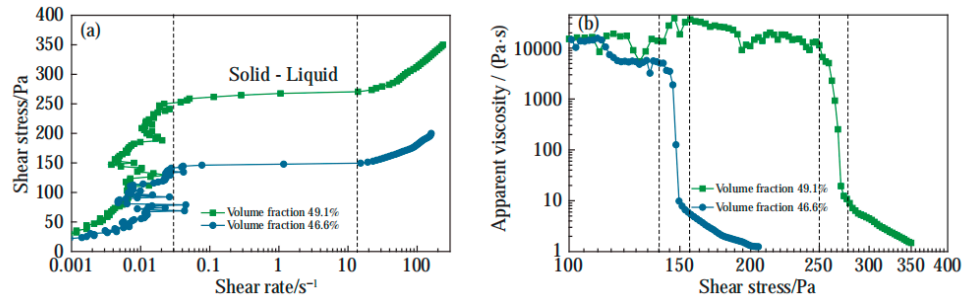


Figure 4: Representative solid–liquid transition behavior of paste systems reported in the literature, illustrating the yield process and structure–controlled transition under different solid volume fractions (adapted from Ref. [12]). (a) Shear stress–shear rate curves; (b) Apparent viscosity–shear stress curves.

From a physical perspective, the yield behavior of paste is not governed by the viscosity of the continuous phase but is primarily controlled by the particulate load-bearing structure formed under high solid volume fraction conditions. As the solid concentration increases, the average interparticle spacing decreases markedly, weakening hydrodynamic lubrication effects and promoting direct particle contacts and frictional interactions. These contacts collectively form a system-spanning mechanical network that enables the paste to sustain external loads in the absence of macroscopic flow [51].

The transition from a solid-like to a fluid-like state does not occur uniformly throughout the paste system but proceeds through progressive structural failure. With increasing applied shear stress, localized rearrangements and instabilities first develop in mechanically weaker regions, giving rise to shear localization. As the stress continues to increase, structural breakdown propagates through the load-bearing network, ultimately resulting in global yielding and sustained flow. This structure-controlled solid–liquid transition explains the spatial heterogeneity and abrupt nature commonly observed during yielding in paste systems. In CPB systems, this structure-controlled yielding is further coupled with cement hydration processes, which progressively modify interparticle bonding and network rigidity over time. This chemo-physical coupling distinguishes CPB from inert suspensions and leads to time-dependent evolution of yield behavior. The structure-controlled yielding of CPB is closely associated with the progressive evolution of particle networks, as schematically illustrated in Fig. 5 (adapted from Ref. [52]).

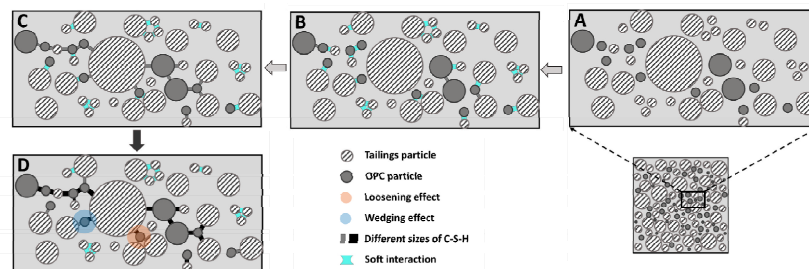


Figure 5: Schematic illustration of the structural evolution of fresh CPB, adapted from Refs. [53,54]. (A) Representative dispersed state of tailings and OPC particles after preshearing. (B) Stage I: flocculation of fine particles into larger agglomerates, accompanied by the initial formation of C–S–H bridges. (C) Stage II: progressive development of rigid interparticle links, leading to an increased number of large agglomerates and a transition from soft colloidal interactions to more rigid contacts. (D) Stage III: continued growth in the size and number of C–S–H bridges, resulting in an increase in system volume, while the overall packing density remains relatively stable due to the combined loosening and wedging effects [52].

Yield stress is not an intrinsic material constant but reflects the instantaneous structural state of the paste. Even for systems with identical compositions, measured yield stress can vary substantially with resting time, preshear history, and loading protocol, highlighting the sensitivity of yield behavior to structural evolution. Across the reviewed studies, reported yield stress values for CPB slurries span several orders of magnitude, primarily due to variations in solid concentration, particle gradation, cement content, curing time, and testing methodology. Under standard rheometer measurements, yield stress values are most commonly reported in the range of 10–100 Pa, whereas substantially higher values, reaching the order of 100–1000 Pa or above, have been observed under specialized conditions such as very high solid contents or fiber-reinforced CPB systems [55–57].

2.2 Shear-Rate-Dependent Nonlinear Rheological Response

Once the applied shear stress exceeds the yield threshold, paste slurry enters a flowing regime in which the apparent viscosity becomes strongly dependent on shear rate, exhibiting pronounced nonlinear rheological behavior. Within most engineering-relevant shear-rate ranges, paste systems predominantly exhibit shear-thinning behavior, characterized by a continuous decrease in apparent viscosity with increasing shear rate [12]. Accordingly, shear-thinning should be regarded as the dominant rheological response of CPB slurries under typical operational conditions, whereas shear-thickening represents a regime-specific behavior that emerges only under extreme combinations of solid fraction, particle contact state, and shear-rate level.

This behavior can be rationalized from the perspective of shear-induced structural evolution. At low to moderate shear rates, the load-bearing structures formed by particle contacts and flocculated aggregates are progressively disrupted by shear, leading to a continuous reduction in the number of structural units capable of transmitting stress and, consequently, a decrease in macroscopic flow resistance. In this regime, shear primarily weakens the internal structure, and structural breakdown dominates the rheological response. In contrast, for pastes with extremely high solid volume fractions or pronounced friction-dominated contact interactions, a transition to shear-thickening behavior has been reported at sufficiently high shear rates [58–61]. Under such conditions, the frequency of instantaneous direct particle contacts increases significantly, accompanied by enhanced frictional dissipation and collisional interactions, resulting in an increase in flow resistance. These observations indicate that the dominant mechanisms governing paste rheology can shift across different shear-rate regimes and material conditions [51].

The coexistence of shear thinning and shear thickening within the same paste system across different shear-rate regimes reflects the competition between structural breakdown mechanisms and particle contact-dominated interactions. This competition gives rise to pronounced nonlinearity and strong system dependence in the rheological response of CPB slurry, making it challenging to describe the flow behavior using a single dominant mechanism or a unified constitutive relation.

2.3 Thixotropic Behavior and Time-Dependent Structural Evolution

Thixotropy refers to the time-dependent and reversible evolution of rheological properties under shear, arising from the breakdown and rebuilding of the internal particle network. In CPB systems, thixotropic behavior is particularly pronounced due to the combined effects of particulate structuring and time-dependent cement hydration.

A key characteristic of thixotropic paste systems is the strong asymmetry between rapid shear-induced structural breakdown and much slower structural rebuilding during rest. Under applied shear, load-bearing particle networks are quickly disrupted, leading to a reduction in apparent viscosity and yield stress.

Upon cessation of shear, the internal structure progressively rebuilds, resulting in a gradual recovery of rheological strength. At short time scales (minutes to hours), thixotropic evolution is primarily governed by physical restructuring of the particle network, including flocculation and contact reformation. At longer time scales (hours to days), cement hydration and setting progressively introduce irreversible chemical bonding, which further increases yield stress and viscosity and may eventually suppress reversibility. This coexistence of reversible physical restructuring and irreversible chemical evolution distinguishes CPB from inert suspensions [62], and is schematically illustrated in Fig. 6 (adapted from Ref. [63]).

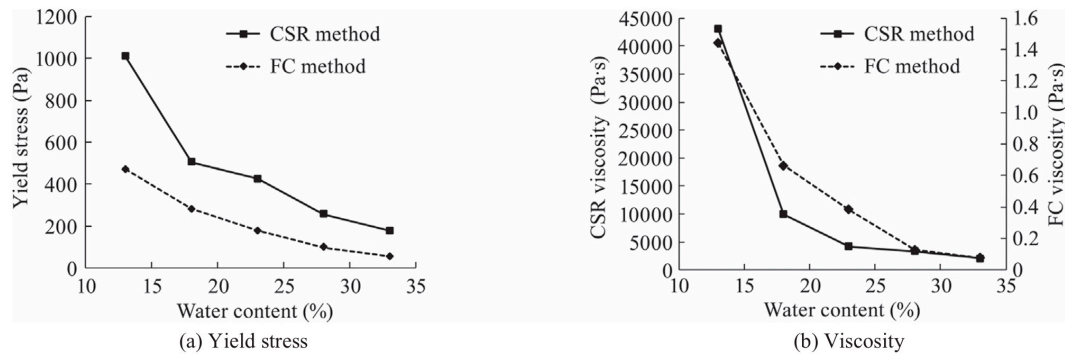


Figure 6: Representative comparison of yield stress and viscosity obtained using constant shear rate (CSR) and flow curve (FC) methods in CPB systems, illustrating the dependence of measured rheological parameters on shear protocol and structural state (adapted from Ref. [63]). (a) Yield stress; (b) Apparent viscosity.

From an engineering perspective, thixotropic structural rebuilding during rest periods can lead to a substantial increase in restart pressure and flow resistance, posing significant challenges for intermittent operation, pipeline restart, and blockage prevention in paste backfill transport systems. This pronounced time dependence underscores the limitations of purely time-independent rheological models and motivates the adoption of structural-parameter-based constitutive frameworks capable of capturing thixotropic evolution and shear-history effects in paste systems.

2.4 Shear History Effects and Differences between Static and Dynamic Yield

The rheological behavior of paste systems is strongly dependent on shear history due to their thixotropic and time-dependent nature. Different shear protocols and resting conditions can therefore lead to substantially different apparent yield stresses, even for identical material compositions [64–66].

Static yield stress is commonly defined as the stress required to initiate flow from a fully rested and structurally rebuilt state, whereas dynamic yield stress corresponds to the stress required to sustain flow after prior shearing has partially disrupted the internal structure. The difference between static and dynamic yield stress reflects distinct structural states induced by different shear histories rather than measurement artifacts [67,68]. Experimental studies consistently report higher static yield stresses than dynamic values, particularly after extended resting periods, owing to progressive structural rebuilding during rest [69,70].

From an engineering perspective, static yield stress is most relevant for pipeline restart, intermittent operation, and blockage risk assessment, while dynamic yield stress is more appropriate for steady-state flow and pressure-drop calculations [71]. This strong dependence on shear history highlights the limitations of time-independent rheological models and motivates the incorporation of structural evolution into constitutive descriptions of paste backfill flow [72,73].

3 Rheological Models for Paste

The rheological behavior of paste slurry is typically non-Newtonian, influenced by factors such as solid particle concentration, binder type, and chemical additives. Commonly used models, such as the Bingham plastic and Herschel-Bulkley models, are effective in describing the flow characteristics of paste under various conditions. Paste flow is governed by yield-stress behavior and, under specific regimes, shear-thickening behavior, where viscosity increases at high shear rates. These models offer practical insights into the paste's flow behavior, which is crucial for applications like mine backfilling and pipeline transport [74,75].

3.1 Bingham Plastic Model

The Bingham plastic model is one of the most widely used rheological models for describing yield-stress fluids [76–79]. This model assumes that the material behaves as a rigid solid when the applied shear stress is lower than a critical yield stress, and begins to flow only after the shear stress exceeds this threshold. The mathematical expression of the Bingham model is given as:

$$\tau = \tau_y + K \dot{\gamma} \quad (1)$$

where τ is the shear stress, τ_y is the yield stress, K is the plastic viscosity, and $\dot{\gamma}$ is the shear rate. The Bingham model characterizes the flow behavior of paste by introducing a yield stress and is widely used to analyze and predict the flow of backfill slurry during pipeline transport.

3.2 Herschel-Bulkley Model

The Herschel–Bulkley model is another widely used rheological model for describing non-Newtonian fluids, particularly those exhibiting yield behavior combined with shear-thinning or shear-thickening characteristics over different shear-rate regimes. The model is expressed as:

$$\tau = \tau_y + K \dot{\gamma}^n \quad (2)$$

where τ is the shear stress, τ_y is the yield stress, K is the consistency index, $\dot{\gamma}$ is the shear rate, and n is the flow behavior index. Compared with the Bingham model, the Herschel–Bulkley model provides greater flexibility in describing the flow behavior of CPB slurry across a wide range of shear rates, particularly in capturing shear-thinning or shear-thickening phenomena at high shear rates. Consequently, this model has been widely applied in the analysis and prediction of paste flow behavior, especially in studies concerning flow resistance and pumping performance.

Experimental studies indicate that paste slurry typically behaves as a yield-stress fluid, and its yield stress is closely related to solid volume fraction, particle morphology, and the presence of chemical additives. Rheological models not only facilitate the optimization of pumping efficiency during pipeline transport but also enable the prediction of slurry flow behavior under different operating conditions. However, because paste rheology is influenced by multiple factors—including solid concentration, binder type, additive usage, particle shape, and particle size distribution—selecting an appropriate rheological model and accurately determining its parameters remain critical for achieving stable and efficient paste backfilling operations.

3.3 Applicability and Limitations of Rheological Models

The applicability of rheological models for paste systems depends on flow conditions, shear history, material composition, and engineering objectives, common non-Newtonian fluid rheological models are presented in Table 1. Model parameters should not be interpreted as intrinsic material constants, but rather as effective descriptors reflecting the instantaneous structural state of the paste under specific testing and operating conditions. Similar conclusions have been drawn in recent slurry pipeline studies, where rheological parameters were shown to vary systematically with solid concentration, particle size distribution, and operating regime, directly affecting pressure loss and energy consumption during transport [80,81].

Conventional viscoplastic models, such as the Bingham and Herschel–Bulkley formulations, remain widely used due to their simplicity and computational convenience. The Bingham model is generally applicable to low shear-rate regimes near yielding, whereas the Herschel–Bulkley model provides greater flexibility in representing nonlinear shear-rate dependence over broader operating ranges [82,83]. These models have been successfully applied to pipeline transport analysis and pressure-drop estimation in dense slurry systems [84]. However, they are inherently local and time-independent, limiting their ability to capture structural evolution, shear-history effects, and transient phenomena such as flow stoppage and restart.

Under flow regimes dominated by time-dependent structural evolution and pronounced thixotropy, structural rheological models incorporating a time-dependent structural parameter (λ) provide a more appropriate framework for describing the progressive build-up and breakdown of internal load-bearing particle networks. Such models have been widely used to interpret stress decay, hysteresis, and flow onset behavior in cementitious and granular suspensions [85,86]. Nevertheless, their application at the pipeline scale remains limited by parameter identifiability and experimental validation, and they should therefore be regarded as complementary rather than universal alternatives to empirical viscoplastic models.

Table 1: A list of non-Newtonian rheological models [12].

Models	Equations
Power-law [87]	$\tau = K(\dot{\gamma})^n$ $n = 1, \text{Newtonian}$ $n < 1, \text{Shear thinning}$ $n > 1, \text{Shear thickening}$ (1)
Bingham [88]	$\begin{cases} \dot{\gamma} = 0, & \tau < \tau_y \\ \tau = \tau_y + \eta_p \dot{\gamma}, & \tau \geq \tau_y \end{cases}$ (2)
Herschel and Bulkley	$\begin{cases} \tau = \tau_y + K(\dot{\gamma})^n, & \tau > \tau_y \\ \dot{\gamma} = 0, & \tau \leq \tau_y \end{cases}$ (3)
Buckingham-Reiner [89]	$\tau_w \approx \frac{\Delta PD}{4L}$ $\tau_w = \eta_p \frac{8v}{D} \left[1 - \frac{4}{3} \left(\tau_y \frac{4L}{\Delta PD} \right) + \frac{1}{3} \left(\tau_y \frac{4L}{\Delta PD} \right)^4 \right]^{-1}$ $\tau_w \approx \frac{4}{3} \tau_y + \eta_p \left(\frac{8v}{D} \right), \quad \text{for } \tau \gg \tau_y$ (4)
Casson [90]	$\sqrt{\tau} = \sqrt{\tau_y} + \sqrt{\eta_c \dot{\gamma}} \quad (\tau > \tau_y) \text{ or } (\tau = \tau_y + \eta_p \dot{\gamma} + 2\sqrt{\tau_y \eta_p \dot{\gamma}})$ $\dot{\gamma} = 0 \quad (\tau \leq \tau_y)$ (5)

4 Factors Influencing the Rheological Properties of Paste

4.1 Effect of Particle Gradation on the Rheological Properties of Paste

Particle gradation plays a significant role in determining the rheological properties of paste, particularly in terms of yield stress and viscosity [57]. From a microstructural perspective, particle size distribution

controls packing efficiency, interparticle contact density, and the balance between lubrication and frictional interactions. Finer particles, with higher specific surface area, tend to increase yield stress by strengthening particle networks. In contrast, coarser particles contribute less to yield stress but predominantly affect the flow resistance at higher shear rates. Accordingly, rheological behavior reflects the combined effects of particle size distribution and solid concentration rather than particle size alone [91].

Experimental studies show that, at comparable solid contents, particle gradation significantly affects both the magnitude and shear-rate dependence of rheological parameters. Incorporation of fine particles (typically $<10\ \mu\text{m}$) has been reported to increase yield stress by approximately 30–40%, while larger particles ($\approx 100\ \mu\text{m}$ and above) primarily influence high-shear flow resistance. Well-graded systems generally exhibit more pronounced shear-thinning due to progressive structural breakdown under shear, whereas poorly graded systems tend to display higher low-shear resistance and weaker shear-thinning behavior [92,93].

From an engineering perspective, particle gradation serves as a practical control parameter for optimizing paste flowability in mine backfilling and pipeline transport. Increasing fines content can improve pumpability and reduce apparent yield stress within appropriate limits, while excessive fines may increase water demand and thixotropy. For cemented paste backfill systems, fines contents on the order of 15–30 wt.% below approximately $20\ \mu\text{m}$ are commonly reported to provide a favorable balance between flowability and structural stability, indicating that optimal gradation design requires balancing improved flow behavior against structural buildup during rest.

4.2 Effect of Temperature on the Rheological Behavior of Paste

Temperature is an important external factor influencing the rheological behavior of cemented paste backfill, particularly yield stress and apparent viscosity. In general, increasing temperature leads to reductions in both yield stress and viscosity at early ages, primarily due to decreased pore fluid viscosity and enhanced particle mobility. Experimental studies have reported that a temperature increase of approximately 10°C can reduce yield stress by 15–20%, although the magnitude of this effect depends on paste composition, solid content, and curing conditions [91]. These observations indicate that temperature directly affects the ease of microstructural rearrangement within the paste [94,95].

From a rheological perspective, the temperature dependence of paste viscosity is often described by Arrhenius-type relationships, reflecting the role of temperature in lowering the energy barrier for structural disruption under shear. At elevated temperatures, particle networks are more readily broken down, resulting in lower apparent viscosity and more pronounced shear-thinning behavior. Conversely, at lower temperatures, reduced thermal motion and stronger interparticle interactions promote higher resistance to flow and may suppress shear-thinning tendencies. These trends highlight that temperature modifies rheological response by regulating the balance between structural stability and shear-induced breakdown [96].

From an engineering standpoint, the influence of temperature on paste rheology has direct implications for mine backfilling and pipeline transport operations. Moderate temperature increases can improve flowability and pumpability during mixing and transport, while prolonged exposure to elevated temperatures accelerates cement hydration and structural buildup, potentially increasing yield stress and thixotropy over time. Accordingly, temperature effects should be interpreted within a time-dependent framework, recognizing that short-term rheological benefits may diminish during extended transport or delayed placement. Effective temperature management therefore represents an important consideration for maintaining consistent paste performance under varying operational conditions [97].

4.3 Effect of Additives on the Rheological Behavior of Paste

Chemical additives and binder-related modifications constitute one of the most extensively studied approaches for controlling CPB rheology [98–100]. Chemical additives, including superplasticizers, dispersants, and mineral admixtures, play an important role in modifying the rheological behavior of paste systems by regulating interparticle interactions and flocculation state [93,101–103]. In general, the addition of suitable chemical admixtures reduces yield stress and apparent viscosity by weakening attractive forces between particles and improving particle dispersion. This effect is particularly pronounced in cemented paste backfill systems, where electrostatic repulsion and steric hindrance introduced by admixtures can significantly alter the load-bearing particle network and promote shear-induced structural breakdown.

Experimental studies consistently report that the effectiveness of additives is strongly dosage-dependent. Within appropriate dosage windows, yield stress reductions on the order of several tens of percent are commonly observed, accompanied by improved shear-thinning behavior and enhanced flowability [67]. However, increasing dosage beyond these optimal ranges often results in diminishing rheological benefits and may induce adverse effects such as segregation, bleeding, or excessive retardation of hydration [63]. These observations highlight that additive performance depends not only on chemical type but also on paste composition, solid concentration, and hydration state. The associated microstructural refinement, characterized by reduced pore connectivity and modified interparticle networks induced by chemical admixtures, is schematically illustrated in Fig. 7 (adapted from Ref. [101]).

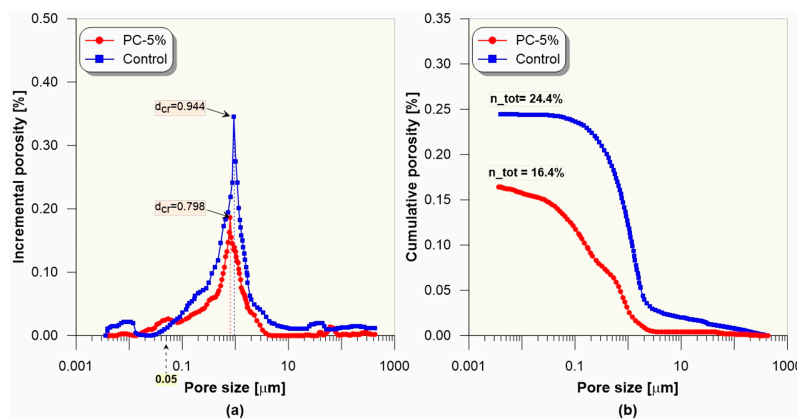


Figure 7: Representative pore-structure refinement induced by superplasticizer addition in cemented paste backfill systems, illustrating changes in pore-size distribution. (a) Incremental pore-size distribution; (b) Cumulative pore-size distribution (adapted from Ref. [101]).

From an engineering perspective, chemical additives provide a practical means for fine-tuning paste rheology to meet specific operational requirements in mine backfilling and pipeline transport. Rather than relying on universal dosage values, the literature emphasizes the importance of dosage optimization tailored to material characteristics and transport conditions. Methodologically, this dosage-design problem can be formulated as a coupled multi-objective optimization task, where rheological controllability, process efficiency, and sustainability-related constraints are balanced simultaneously [104]. When applied within appropriate ranges, additives can effectively enhance pumpability and transport stability, whereas improper selection or overdosing may compromise paste uniformity and long-term performance.

5 Challenges and Emerging Directions in Paste Rheology

5.1 Challenges of Nonlocal Effects in Paste Rheology Behavior

A large body of experimental and numerical studies has demonstrated that paste materials often exhibit pronounced spatially heterogeneous flow behaviors under shear, including shear localization, plug flow, and the coexistence of flowing regions with quasi-static zones. Although these phenomena have been extensively observed, their underlying formation mechanisms and their influence on macroscopic rheological behavior remain poorly unified. Existing studies generally agree that such spatially heterogeneous flows cannot be adequately explained solely by local shear rate or stress conditions, but are closely related to the spatial distribution and evolution of the internal microstructure of the system [14]. Local structural rearrangements and changes in particle contact states may influence neighboring regions through stress transmission, thereby inducing strong spatial coupling in the flow behavior [21,105]. In this context, traditional rheological models based on purely local constitutive assumptions often fail to effectively capture these heterogeneous flow characteristics in highly concentrated paste systems [106]. In recent years, some studies have attempted to address this issue by introducing structural evolution variables or gradient correction terms, however, the physical interpretability and applicability range of these models still require further validation. Consequently, the development of a rheological theoretical framework capable of consistently describing both structural evolution and spatially heterogeneous flow remains one of the key challenges in this field.

5.2 Scale Effects and Experimental–Model Consistency

Previous studies have consistently shown that the rheological response of paste materials is highly sensitive to experimental scale, shear configuration, and loading history, which is widely recognized as a major factor limiting the general applicability of yield-stress-based rheological models [107–110]. Even for paste systems with identical material compositions, substantial variations in macroscopic parameters, such as yield stress and apparent viscosity, can emerge under different geometrical dimensions, shear modes, and boundary conditions [108,111]. Mechanistically, these discrepancies are generally attributed to the coupling between internal structural length scales and external flow or observation scales [112–116]. When the system size approaches or falls below the dominant structural length scale, local heterogeneities are amplified, and the macroscopic response may deviate markedly from classical continuum assumptions; by contrast, at larger scales, local structural effects are partially averaged out, resulting in apparently more homogeneous flow behavior [117–120]. Therefore, explicitly incorporating the interactions among structural length scales, temporal scales, and experimental observation scales is a central scientific challenge for achieving cross-condition consistency and improving predictive capability [121–125]. Recent advances in multiscale constitutive modeling and predictive rheological frameworks further support this direction [126–130].

5.3 From Empirical Descriptions to a Unified Physical Framework

Overall, research on the rheology of highly concentrated pastes is gradually shifting from predominantly empirical, curve-fitting-based descriptive models toward unified theoretical frameworks constrained by physical mechanisms [131–134]. Existing studies indicate that this transition does not rely on continuously increasing model complexity, but rather requires the rational incorporation of the intrinsic relationships among key physical factors such as microstructural evolution and scale effects during model development. The literature suggests that merely introducing more complex constitutive formulations often fails to fundamentally enhance model applicability across different material systems and

flow conditions [135]. A complementary strategy is to use dual-perspective influence screening to detect key interaction pathways among variables prior to model fitting, which helps reduce redundant complexity while retaining dominant system-level effects [136]. In contrast, describing the formation, breakdown, and reorganization of dominant internal structures using a limited number of state variables with clear physical meaning is considered a more promising pathway toward achieving both model unification and experimental verifiability. Consequently, future developments in paste rheology should focus on establishing a reasonable balance between experimental observability and model simplicity, and on this basis, constructing physically consistent frameworks capable of capturing flow behavior across multiple scales. This research direction is widely recognized as a critical foundation for advancing paste rheology from empirical analysis toward quantitative prediction [137–141].

5.4 Applications of Artificial Intelligence in Paste Rheology

In recent years, data-driven methodologies have been increasingly introduced into the rheological study of complex fluids and dense particulate systems as a complement to traditional physics-based modeling approaches [142–144]. Machine learning techniques are particularly effective in handling high-dimensional input spaces and strongly nonlinear relationships, enabling the establishment of empirical mappings between material composition, microstructural characteristics, and macroscopic rheological responses. In paste rheology, supervised learning models have been widely applied to correlate mixture proportions and experimental conditions with key rheological parameters such as yield stress and apparent viscosity, thereby reducing experimental workload and improving parameter-screening efficiency [145]. In addition, data-driven frameworks have been used to jointly analyze experimental data and numerical simulation results, allowing multivariate sensitivity assessment and identification of dominant factors governing flow behavior [146,147].

To enhance physical consistency and practical relevance, recent studies have increasingly integrated machine learning with rheological principles by embedding physical constraints or structural descriptors into learning frameworks. Such physics-constrained approaches, including physics-informed neural networks (PINNs), aim to preserve mechanically plausible trends while improving predictive robustness, and are particularly attractive for multiscale rheological problems that are difficult to capture using conventional constitutive models alone [148,149]. In applications relevant to paste and CPB systems, these frameworks typically rely on multi-source data integration, combining laboratory rheometry, field-scale transport records, and routine operational variables such as solid concentration, temperature, resting time, and shear history, thereby improving reproducibility and transferability across material systems and operating conditions [150,151]. Physical bounds and rheological consistency constraints are introduced to control extrapolation behavior and suppress nonphysical predictions beyond the training domain [152,153].

Recent developments further emphasize interpretable feature construction, structured learning strategies, and optimization-based calibration to enhance model stability and identifiability under industrial data conditions [154,155]. From an engineering perspective, uncertainty quantification and reliability-oriented validation have become essential components for deploying data-driven rheological models in mine backfilling operations. Model outputs are increasingly linked to decision-oriented tasks, including mix-design screening, pumpability-window identification, pressure-loss risk monitoring, and restart-risk assessment following flow interruption, forming an integrated “input–learning–validation–decision” workflow [156,157]. Representative data-driven and physics-informed modeling frameworks reported in the literature, including sequence-based learning models and physics-informed neural networks, illustrate transferable strategies for linking complex rheological responses with underlying physical constraints [158].

Fig. 8 summarizes commonly reported elements in the literature, including multi-source inputs, physics-constrained learning, unified validation, and engineering mapping, and organizes them into a conceptual framework relevant to paste rheology. Despite their demonstrated potential, existing studies also highlight limitations of artificial intelligence approaches, particularly with respect to interpretability, extrapolation capability, and dependence on data quality. Addressing these challenges will require further development of hybrid modeling strategies that more tightly integrate data-driven techniques with fundamental rheological principles, thereby improving both predictive reliability and mechanistic understanding in practical applications [159,160].

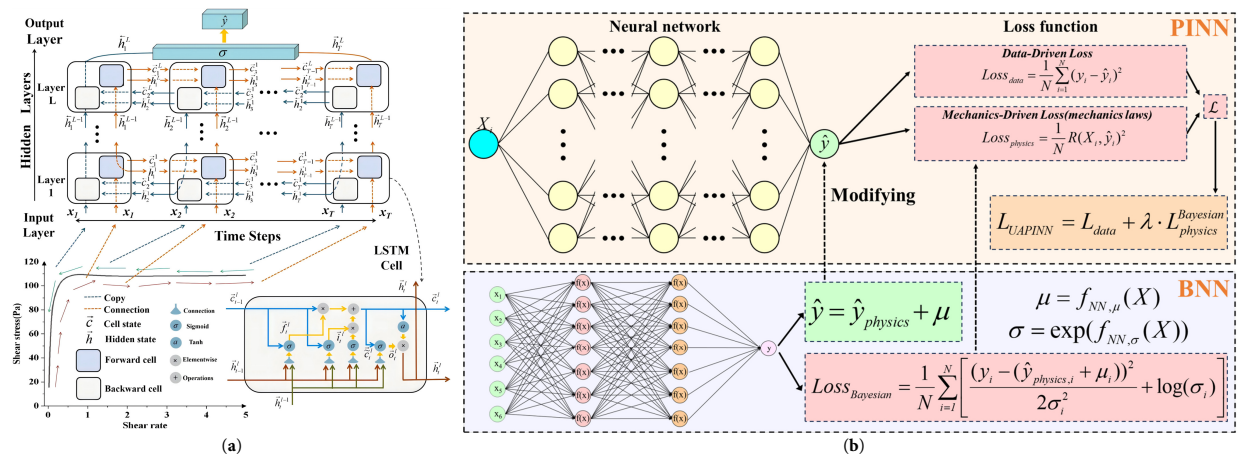


Figure 8: Representative data-driven and physics-informed modeling frameworks reported in the literature for complex geophysical and rheological systems (adapted from Ref. [157]). (a) A bidirectional long short-term memory (BiLSTM)-based model for debris-flow rheology prediction, illustrating sequence-based learning of shear-rate–shear-stress relationships. (b) A physics-informed neural network (PINN) framework for rock-strength prediction, in which data-driven learning is coupled with mechanics-based constraints to ensure physically consistent predictions.

6 Conclusions and Future Perspectives

Paste rheology in mine backfilling systems is governed by the coupled effects of particulate structure, time-dependent structural evolution, spatial heterogeneity, and scale dependence. From a structure-controlled perspective that accounts for nonlocal effects and observation scale, this review synthesizes experimental evidence, rheological models, and emerging data-driven approaches, highlighting the challenges of reconciling results across different material systems and testing conditions. The main conclusions and future perspectives can be summarized as follows.

- (1) The macroscopic flow behavior of paste is primarily controlled by the formation and evolution of internal particle networks, rather than by the properties of the liquid phase alone.
- (2) Empirical constitutive models widely used in practice provide useful engineering approximations under specific flow conditions, such as steady-state transport in shallow or well-controlled mining systems. However, they are limited in describing structural evolution, time dependence, and spatially heterogeneous flow behavior that commonly arise in deeper or more complex mining operations, where high pressure, flow interruption, and restart conditions are prevalent.
- (3) Rheological parameters are strongly influenced by testing protocols and observation scale, underscoring the need for improved experimental consistency and scale-aware interpretation.

- (4) Particle gradation, temperature, and additives modify paste rheology by altering interparticle interactions and hydration processes, offering practical means of rheological control for optimizing pumpability and transport stability when applied appropriately.
- (5) There remains a lack of rheological models capable of consistently linking microstructural evolution with macroscopic flow behavior across relevant length and time scales, particularly in capturing structure-controlled yielding, spatial heterogeneity, and scale dependence.
- (6) Data-driven and physics-informed approaches show promise for modeling history-dependent rheological behavior, but their broader application is limited by challenges in interpretability, robustness, and integration with physical mechanisms.

Acknowledgement: Not applicable.

Funding Statement: This research was funded by The Seed Fund Cultivation Project of Ocean College, Zhejiang University (2025BS002) and A Project Supported by Scientific Research Fund of Zhejiang University (XY2025056).

Author Contributions: The authors confirm contribution to the paper as follows: Conceptualization, Mingzhi Zhang and Haonan Zhang; methodology, Tianxing Ma and Yun Lin; software, Qian Zhang; validation, Mingzhi Zhang, Xionghuan Tan and Tianxing Ma; formal analysis, Liangxu Shen; investigation, Haonan Zhang; resources, Xuecheng Shang; data curation, Haonan Zhang; writing—original draft preparation, Mingzhi Zhang; writing—review and editing, Tianxing Ma; visualization, Junwei Shu and Zheyuan Jiang; supervision, Liangxu Shen; project administration, Tianxing Ma; funding acquisition, Tianxing Ma. All authors reviewed and approved the final version of the manuscript.

Availability of Data and Materials: The data that support the findings of this study are available from the Corresponding Author, [Tianxing Ma], upon reasonable request.

Ethics Approval: Not applicable.

Conflicts of Interest: The authors declare no conflicts of interest.

References

1. Santamarina JC, Torres-Cruz LA, Bachus RC. Why coal ash and tailings dam disasters occur. *Science*. 2019;364(6440):526–8. [[CrossRef](#)].
2. Wang L, Wu AX, Ruan ZE, Wang SY, Wang JD. Rheological properties and prediction model of trans-scale cemented paste backfill slurry. *Chin J Nonferrous Met*. 2025;35(11):3960–73. (In Chinese). [[CrossRef](#)].
3. Wang C, Harbottle D, Liu Q, Xu Z. Current state of fine mineral tailings treatment: A critical review on theory and practice. *Min Eng*. 2014;58:113–31. [[CrossRef](#)].
4. Qi C, Fourie A. Cemented paste backfill for mineral tailings management: Review and future perspectives. *Min Eng*. 2019;144:106025. [[CrossRef](#)].
5. Belem T, Benzaazoua M. Design and application of underground mine paste backfill technology. *Geotech Geol Eng*. 2008;26(2):147–74. [[CrossRef](#)].
6. Wu A. *Rheology of Paste in Metal Mines*. Singapore: Springer; 2022 [[CrossRef](#)].
7. Yin S, Shao Y, Wu A, Wang H, Liu X, Wang Y. A systematic review of paste technology in metal mines for cleaner production in China. *J Clean Prod*. 2020;247:119590. [[CrossRef](#)].
8. Wu AX, Yang Y, Cheng HY, Chen SM, Han Y. Status and prospects of paste technology in China. *Chin J Eng*. 2018;40(5):517–25.
9. Pullum L, Boger DV, Sofra F. Hydraulic mineral waste transport and storage. *Annu Rev Fluid Mech*. 2018;50:157–85. [[CrossRef](#)].
10. Fehrsen M, Cooke R. Paste fill pipeline distribution systems-current status. *Rise Mchines State Art Min Mech Autom Hydraul Transp Commun*. 2006:1–13.

11. Wu A, Ruan Z, Wang J. Rheological behavior of paste in metal mines. *Int J Min Met Mater*. 2022;29(4):717–26. [[CrossRef](#)].
12. Wu AX, Li H, Cheng HY, Wang YM, Li CP, Ruan ZE. Status and prospects of researches on rheology of paste backfill using unclassified-tailings (Part 1): Concepts, characteristics and models. *Chin J Eng*. 2020;42(7):803–13.
13. Coussot P. *Rheometry of Pastes, Suspensions, and Granular Materials: Applications in Industry and Environment*. Hoboken, NJ, USA: John Wiley & Sons, Inc.; 2005. [[CrossRef](#)].
14. Mewis J, Wagner NJ. Thixotropy. *Adv Colloid Interface Sci*. 2009;147–148:214–27. [[CrossRef](#)].
15. Feys D, Cepuritis R, Jacobsen S, Lesage K, Secrieru E, Yahia A. Measuring rheological properties of cement pastes: Most common techniques, procedures and challenges. *RILEM Tech Lett*. 2017;2:129–35. [[CrossRef](#)].
16. Mbasha W, Masalova I, Haldenwang R, Malkin A. The yield stress of cement pastes as obtained by different rheological approaches. *Cape Penins Univ Technol*. 2015.
17. Knight A, Sofrà F, Stickland A, Scales P, Lester D, Buscall R. Variability of shear yield stress—measurement and implications for mineral processing. *Proc 20th Int Semin Paste Thick Tailings*. 2017:57–65. [[CrossRef](#)].
18. Buscall R, White LR. The consolidation of concentrated suspensions. Part 1.—The theory of sedimentation. *J Chem Soc Faraday Trans 1*. 1987;83(3):873. [[CrossRef](#)].
19. Barnes HA. The yield stress—A review or ‘ $\pi\alpha\nu\tau\alpha$ ρει’—Everything flows? *J Non Newton Fluid Mech*. 1999;81(1–2):133–78. [[CrossRef](#)].
20. Pullum L, Graham L, Rudman M, Hamilton R. High concentration suspension pumping. *Min Eng*. 2006;19(5):471–7. [[CrossRef](#)].
21. Kalyon DM. Apparent slip and viscoplasticity of concentrated suspensions. *J Rheol*. 2005;49(3):621–40. [[CrossRef](#)].
22. Goyon J, Colin A, Ovarlez G, Ajdari A, Bocquet L. Spatial cooperativity in soft glassy flows. *Nature*. 2008;454(7200):84–7. [[CrossRef](#)].
23. Bocquet L, Colin A, Ajdari A. Kinetic theory of plastic flow in soft glassy materials. *Phys Rev Lett*. 2009;103(3):036001. [[CrossRef](#)].
24. Kamrin K, Koval G. Nonlocal constitutive relation for steady granular flow. *Phys Rev Lett*. 2012;108(17):178301. [[CrossRef](#)].
25. Kamrin K, Henann DL. Nonlocal modeling of granular flows down inclines. *Soft Matter*. 2015;11(1):179–85. [[CrossRef](#)].
26. Ruan Z, Wu A, Bürger R, Betancourt F, Wang Y, Wang Y, et al. Effect of interparticle interactions on the yield stress of thickened flocculated copper mineral tailings slurry. *Powder Technol*. 2021;392:278–85. [[CrossRef](#)].
27. Navarrete I, La Fé-Perdomo I, Ramos-Grez JA, Lopez M. Predicting the evolution of static yield stress with time of blended cement paste through a machine learning approach. *Constr Build Mater*. 2023;371:130632. [[CrossRef](#)].
28. Nazar S, Yang J, Faisal Javed M, Khan K, Li L, Liu QF. An evolutionary machine learning-based model to estimate the rheological parameters of fresh concrete. *Structures*. 2023;48:1670–83. [[CrossRef](#)].
29. Karniadakis GE, Kevrekidis IG, Lu L, Perdikaris P, Wang S, Yang L. Physics-informed machine learning. *Nat Rev Phys*. 2021;3(6):422–40. [[CrossRef](#)].
30. Chen H, Ma T, Shen L, Liu Z, Ni S, Sun H. Assessment of debris flow susceptibility based on PCA-IVCoupling method and SHAP Model: A case study of Linan District. *Trans GIS*. 2025;29(7):e70146. [[CrossRef](#)].
31. Wang Y, Ma T, Shen L, Wang X, Luo R. Prediction of thermal conductivity of natural rock materials using LLE-transformer-lightGBM model for geothermal energy applications. *Energy Rep*. 2025;13:2516–30. [[CrossRef](#)].
32. Canbek O, Xu Q, Mei Y, Washburn NR, Kurtis KE. Predicting the rheology of limestone calcined clay cements (LC3): Linking composition and hydration kinetics to yield stress through Machine Learning. *Cem Concr Res*. 2022;160:106925. [[CrossRef](#)].
33. Şahin HG, Altun ÖB, Eser M, Mardani A, Bilgin M. Research on modeling the thixotropic properties of cementitious systems using regression methods in machine learning. *Constr Build Mater*. 2024;411:134633. [[CrossRef](#)].
34. Lin Y, Guo Z, Meng Q, Li C, Ma T. Prediction of peak strength under triaxial compression for sandstone based on ABC-SVM algorithm. *Expert Syst Appl*. 2025;264:125923. [[CrossRef](#)].
35. Liu H, Ma T, Lin Y, Peng K, Hu X, Xie S, et al. Deep learning in rockburst intensity level prediction: Performance evaluation and comparison of the NGO-CNN-BiGRU-attention model. *Appl Sci*. 2024;14(13):5719. [[CrossRef](#)].

36. Wang T, Ge Q, Ma T, Chen H, Luo R, Wang X, et al. A novel method for predicting debris flow hazard: A multi-strategy fusion approach based on the light gradient boosting machine framework. *Stoch Environ Res Risk Assess.* 2025;39(10):4867–90. [[CrossRef](#)].
37. Davoodi S, Mehrad M, Wood DA, Ghorbani H, Rukavishnikov VS. Hybridized machine-learning for prompt prediction of rheology and filtration properties of water-based drilling fluids. *Eng Appl Artif Intell.* 2023;123:106459. [[CrossRef](#)].
38. Ruan Y, Qin X, Liu S, Zhang M, Tang J, Guo Y, et al. GRAIN: Gravity-resistance adaptive framework for identifying influential nodes using multi-order structural diversity. *Inf Process Manag.* 2026;63(4):104618. [[CrossRef](#)].
39. Wahab S, Salami BA, AlAteah AH, Al-Tholaia MMH, Alahmari TS. Exploring the interrelationships between composition, rheology, and compressive strength of self-compacting concrete: An exploration of explainable boosting algorithms. *Case Stud Constr Mater.* 2024;20:e03084. [[CrossRef](#)].
40. Peng K, Luo K, Wang Y, Luo S, Ma T, Mao J, et al. Stress wave propagation and energy characteristics of impact-damaged and water-soaked sandstone with different length-to-diameter ratios. *J Rock Mech Geotech Eng.* 2025:1–16. [[CrossRef](#)].
41. Li Z. Toward low-carbon construction: A review of red mud utilization in cementitious materials and geopolymers for sustainability and cost benefits. *Buildings.* 2026;16(2):362. [[CrossRef](#)].
42. Ciutara CO, Barman S, Iasella S, Huang B, Zasadzinski JA. Dilatational and shear rheology of soluble and insoluble monolayers with a Langmuir trough. *J Colloid Interface Sci.* 2023;629(Pt A):125–35. [[CrossRef](#)].
43. Xie S, Jiang Z, Lin H, Ma T, Peng K, Liu H, et al. A new integrated intelligent computing paradigm for predicting joints shear strength. *Geosci Front.* 2024;15(6):101884. [[CrossRef](#)].
44. Xie S, Lin H, Ma T, Peng K, Sun Z. Prediction of joint roughness coefficient *via* hybrid machine learning model combined with principal components analysis. *J Rock Mech Geotech Eng.* 2025;17(4):2291–306. [[CrossRef](#)].
45. Cacciuttolo C, Marinovic A. Experiences of underground mine backfilling using mine tailings developed in the Andean Region of Peru: A green mining solution to reduce socio-environmental impacts. *Sustainability.* 2023;15(17):12912. [[CrossRef](#)].
46. Hustrulid WA, Bullock RL, editors. *Underground mining methods: Engineering fundamentals and international case studies.* Littleton, CO, USA: SME; 2001.
47. Kesimal A, Yilmaz E, Ercikdi B. Evaluation of paste backfill mixtures consisting of sulphide-rich mill tailings and varying cement contents. *Cem Concr Res.* 2004;34(10):1817–22. [[CrossRef](#)].
48. Jiao HZ. Research of paste new definition from the viewpoint of saturation ratio and bleeding rate. *J Wuhan Univ Technol.* 2011;33(6):85–9
49. Ling W, Chen J, Ma W. Study on the rheological properties of high calcium desulfurization ash-slag-based paste backfill material. *Appl Sci.* 2025;15(9):5105. [[CrossRef](#)].
50. Hefni MA. Investigating the basic properties of basalt fiber reinforced cemented paste backfill as a sustainable material for mine backfilling. *Sci Rep.* 2025;15(1):10073. [[CrossRef](#)].
51. Li Q, Wang B, Liu C, Kang M, Yang L. Rheological and thixotropic properties of cemented ultrafine tailings backfill with cold-bonded lightweight aggregates. *Powder Technol.* 2025;455:120750. [[CrossRef](#)].
52. Guo Z, Qiu J, Pel L, Zhao Y, Zhu Q, Kwek JW, et al. A contribution to understanding the rheological measurement, yielding mechanism and structural evolution of fresh cemented paste backfill. *Cem Concr Compos.* 2023;143:105221. [[CrossRef](#)].
53. Roussel N, Ovarlez G, Garrault S, Brumaud C. The origins of thixotropy of fresh cement pastes. *Cem Concr Res.* 2012;42(1):148–57. [[CrossRef](#)].
54. Wallevik JE. Rheological properties of cement paste: Thixotropic behavior and structural breakdown. *Cem Concr Res.* 2009;39(1):14–29. [[CrossRef](#)].
55. Yowa GG, Sivakugan N, Tuladhar R, Arpa G. Strength and rheology of cemented pastefill using waste pitchstone fines and common pozzolans compared to using Portland cement. *Int J Geosynth Ground Eng.* 2022;8(5):56. [[CrossRef](#)].
56. Ouyang J, Corr DJ, Shah SP. Factors influencing the rheology of fresh cement asphalt emulsion paste. *J Mater Civ Eng.* 2016;28(11):04016140. [[CrossRef](#)].
57. Silva M, Hansson M, eSilva MC. Rheological yield stress measurement of paste fill: New technical approaches. In: *Minefill 2020-2021.* Boca Raton, FL, USA: CRC Press; 2021. p. 169–82. [[CrossRef](#)].

58. Yang L, Wang H, Wu A, Li H, Tchamba AB, Bier TA. Shear thinning and thickening of cemented paste backfill. *Appl Rheol*. 2019;29(1):80–93. [[CrossRef](#)].
59. Wyart M, Cates ME. Discontinuous shear thickening without inertia in dense non-Brownian suspensions. *Phys Rev Lett*. 2014;112(9):098302. [[CrossRef](#)].
60. Guy BM, Ness C, Hermes M, Sawiak LJ, Sun J, Poon WCK. Testing the Wyart-Cates model for non-Brownian shear thickening using bidisperse suspensions. *Soft Matter*. 2020;16(1):229–37. [[CrossRef](#)].
61. Martys NS, George WL, Chun BW, Lootens D. A smoothed particle hydrodynamics-based fluid model with a spatially dependent viscosity: Application to flow of a suspension with a non-Newtonian fluid matrix. *Rheol Acta*. 2010;49(10):1059–69. [[CrossRef](#)].
62. Roshani A, Fall M. Flow ability of cemented pastefill material that contains nano-silica particles. *Powder Technol*. 2020;373:289–300. [[CrossRef](#)].
63. Zhao Y, Taheri A, Karakus M, Chen Z, Deng A. Effects of water content, water type and temperature on the rheological behaviour of slag-cement and fly ash-cement paste backfill. *Int J Min Sci Technol*. 2020;30(3):271–8. [[CrossRef](#)].
64. Dhar S, Liberto T, Barentin C, Divoux T, Robisson A. Discrepancies in dynamic yield stress measurements of cement pastes. *Rheol Acta*. 2024;63(9):657–72. [[CrossRef](#)].
65. Guo Z, Qiu J, Jiang H, Zhu Q, Wang Kwek J, Ke L, et al. Experimental and modeling study on the transient flow and time-dependent yield stress of superfine-tailings cemented paste backfill. *Constr Build Mater*. 2023;367:130363. [[CrossRef](#)].
66. Nguyen QD, Boger DV. Thixotropic behaviour of concentrated bauxite residue suspensions. *Rheol Acta*. 1985;24(4):427–37. [[CrossRef](#)].
67. Yin S, Wu A, Hu K, Wang Y, Zhang Y. The effect of solid components on the rheological and mechanical properties of cemented paste backfill. *Min Eng*. 2012;35:61–6. [[CrossRef](#)].
68. Cheng H, Wu S, Li H, Zhang X. Influence of time and temperature on rheology and flow performance of cemented paste backfill. *Constr Build Mater*. 2020;231:117117. [[CrossRef](#)].
69. Qian Y, Kawashima S. Distinguishing dynamic and static yield stress of fresh cement mortars through thixotropy. *Cem Concr Compos*. 2018;86:288–96. [[CrossRef](#)].
70. Abedi B, Marín Castaño EP, C Rodrigues E, Thompson RL, de Souza Mendes PR. Obtaining test-independent values of the dynamic and static yield stresses for time-dependent materials. *Rheol Acta*. 2023;62(11):665–85. [[CrossRef](#)].
71. Moisés GVL, Alencar LS, Naccache MF, Frigaard IA. The influence of thixotropy in start-up flow of yield stress fluids in a pipe. *J Pet Sci Eng*. 2018;171:794–807. [[CrossRef](#)].
72. Wang XL, Wang HJ, Wu AX, Jiang HQ, Peng QS, Zhang X. Evaluation of time-dependent rheological properties of cemented paste backfill incorporating superplasticizer with special focus on thixotropy and static yield stress. *J Cent South Univ*. 2022;29(4):1239–49. [[CrossRef](#)].
73. Yusufi BK, Kapelan Z, Mehta D. Advances in modeling the flow of Herschel–Bulkley fluids in pipes: A review. *Phys Fluids*. 2025;37(2):021302. [[CrossRef](#)].
74. Nehdi M, Rahman MA. Estimating rheological properties of cement pastes using various rheological models for different test geometry, gap and surface friction. *Cem Concr Res*. 2004;34(11):1993–2007. [[CrossRef](#)].
75. Campos RS, Maciel GF. Test protocol and rheological model influence on determining the rheological properties of cement pastes. *J Build Eng*. 2021;44:103206. [[CrossRef](#)].
76. Lampaert SGE, van Ostayen RAJ. Lubrication theory for Bingham plastics. *Tribol Int*. 2020;147:106160. [[CrossRef](#)].
77. Galarce F, Martinez F. A parametric study of the pipeline hammer phenomenon in plastic Bingham slurry flows using the finite element method. *J Eng Math*. 2025;153(1):9. [[CrossRef](#)].
78. Shen L, Ma T, Chen H, Ye B, Luo R, Sun H. A new CNN-GRU deep learning framework optimized by CHIO for precise prediction of debris flow velocity. *Stoch Environ Res Risk Assess*. 2025;39(6):2351–71. [[CrossRef](#)].
79. Ma T, Luo R, Shen L, Ye B, Wang X, Sun H. Modified Herschel–Bulkley–Papanastasiou model considering particle size distribution to debris flow rheological properties. *Phys Fluids*. 2025;37(2):023127. [[CrossRef](#)].
80. Pradhan AR, Kumar S. Enhancing the flowability of limestone water suspension for economical transportation by variation in particle size distribution. *Part Sci Technol*. 2024;42(1):31–48. [[CrossRef](#)].

81. Pradhan AR. Rheology-driven approaches in slurry transportation: Influence of bimodal mixtures, additives, and modelling perspectives. *Adv Colloid Interface Sci.* 2026;347:103714. [[CrossRef](#)].
82. Wang D, Barakos G, Cheng Z, Mischo H, Zhao J. Numerical simulation of pressure profile of mining backfill fly-ash slurry in an L-shaped pipe using a validated Herschel-Bulkley model. *J Sustain Cem Based Mater.* 2023;12(3):219–33. [[CrossRef](#)].
83. Castro M, Giles DW, Macosko CW, Moaddel T. Comparison of methods to measure yield stress of soft solids. *J Rheol.* 2010;54(1):81–94. [[CrossRef](#)].
84. Gupta C, Kumar S, Pradhan AR. Role of nonionic natural dispersing agent *Acacia Concinna* on the slurryability and stability of concentrated iron ore suspension. *Chem Eng Commun.* 2024;211(7):1043–60. [[CrossRef](#)].
85. Roussel N. A thixotropy model for fresh fluid concretes: Theory, validation and applications. *Cem Concr Res.* 2006;36(10):1797–806. [[CrossRef](#)].
86. Qian Y, Kawashima S. Flow onset of fresh mortars in rheometers: Contribution of paste deflocculation and sand particle migration. *Cem Concr Res.* 2016;90:97–103. [[CrossRef](#)].
87. Atzeni C, Massidda L, Sanna U. Comparison between rheological models for Portland cement pastes. *Cem Concr Res.* 1985;15(3):511–9. [[CrossRef](#)].
88. Bingham BEC. *Fluidity and Plasticity*. New York, NY, USA: McGraw-Hill; 1922.
89. Buckingham E. On plastic flow through capillary tubes. *Proc Am Soc Test Mater.* 1921;29(21):1154–56.
90. Casson N. A flow equation for pigment-oil suspensions of the printing ink type. *Rheol Disperse Syst.* 1959:84–104.
91. Cheng HY, Wu SC, Zhang XQ, Wu AX. Effect of particle gradation characteristics on yield stress of cemented paste backfill. *Int J Min Met Mater.* 2020;27(1):10–7. [[CrossRef](#)].
92. Gupta S, Tulliani JM, Kua HW. Carbonaceous admixtures in cementitious building materials: Effect of particle size blending on rheology, packing, early age properties and processing energy demand. *Sci Total Environ.* 2022;807(Pt 2):150884. [[CrossRef](#)].
93. Ouattara D, Yahia A, Mbonimpa M, Belem T. Effects of superplasticizer on rheological properties of cemented paste backfills. *Int J Min Process.* 2017;161:28–40. [[CrossRef](#)].
94. Hu B, Hu X, Lin C, Du G, Ma T, Li K. Evolution of physical and mechanical properties of granite after thermal treatment under cyclic uniaxial compression. *Sustainability.* 2023;15(18):13676. [[CrossRef](#)].
95. Wang Y, Luo K, Peng K, Wu Q, Luo S, Ma T, et al. Experimental study of the dynamic tensile properties of water-saturated sandstone with different length-to-diameter ratios. *Soil Dyn Earthq Eng.* 2025;190:109191. [[CrossRef](#)].
96. Banfill PFG, Rodríguez O, de Rojas MS, Frías M. Effect of activation conditions of a kaolinite based waste on rheology of blended cement pastes. *Cem Concr Res.* 2009;39(10):843–8. [[CrossRef](#)].
97. Nguty TA, Ekere NN. Modeling the effects of temperature on the rheology of solder pastes and flux system. *J Mater Sci Mater Electron.* 2000;11(1):39–43. [[CrossRef](#)].
98. Che C, Bi YZ, Sun XP, Feng Z, Ma TX, Jiang ZY, et al. Hydraulic performance of polymer-amended bentonite for containment of zinc-contaminated groundwater. *Environ Earth Sci.* 2025;84(20):565. [[CrossRef](#)].
99. Arizzi A, Banfill PFG. Rheology of lime pastes with biopolymer-based additives. *Mater Struct.* 2019;52(1):8. [[CrossRef](#)].
100. Bressi S, Carter A, Bueche N, Dumont AG. Impact of different ageing levels on binder rheology. *Int J Pavement Eng.* 2016;17(5):403–13. [[CrossRef](#)].
101. Cavusoglu I. Superplasticizer dosage effect on strength, microstructure and permeability enhancement of cementitious paste fills. *Minerals.* 2024;14(12):1242. [[CrossRef](#)].
102. Airey GD, Mohammed MH. Rheological properties of polyacrylates used as synthetic road binders. *Rheol Acta.* 2008;47(7):751–63. [[CrossRef](#)].
103. Jiao D, Lesage K, Yardimci MY, Shi C, De Schutter G. Possibilities of fly ash as responsive additive in magneto-rheology control of cementitious materials. *Constr Build Mater.* 2021;296:123656. [[CrossRef](#)].
104. Xu YP, Lin ZH, Ma TX, She C, Xing SM, Qi LY, et al. Optimization of a biomass-driven Rankine cycle integrated with multi-effect desalination, and solid oxide electrolyzer for power, hydrogen, and freshwater production. *Desalination.* 2022;525:115486. [[CrossRef](#)].

105. Barnes HA. Shear-thickening (“dilatancy”) in suspensions of nonaggregating solid particles dispersed in Newtonian liquids. *J Rheol.* 1989;33(2):329–66. [[CrossRef](#)].
106. Barnes HA, Nguyen QD. Rotating vane rheometry—A review. *J Non Newton Fluid Mech.* 2001;98(1):1–14. [[CrossRef](#)].
107. Fall A, Bertrand F, Ovarlez G, Bonn D. Shear thickening of cornstarch suspensions. *J Rheol.* 2012;56(3):575–91. [[CrossRef](#)].
108. Coussot P, Ovarlez G. Physical origin of shear-banding in jammed systems. *Eur Phys J E Soft Matter.* 2010;33(3):183–8. [[CrossRef](#)].
109. Yang S, Meng D, Diaz A, Yang H, Su X, de Jesus AMP. Probabilistic modeling of uncertainties in reliability analysis of mid- and high-strength steel pipelines under hydrogen-induced damage. *Int J Struct Integr.* 2025;16(1):39–59. [[CrossRef](#)].
110. Meng D, Nie P, Yang S, Su X, Liao C. Reliability analysis of wind turbine gearboxes: Past, progress and future prospects. *Int J Struct Integr.* 2025;16(1):4–38. [[CrossRef](#)].
111. Wang Q, Ma T, Yang S, Yan F, Zhao J. Intelligent rockburst level prediction model based on swarm intelligence optimization and multi-strategy learner soft voting hybrid ensemble. *Geomech Geophys Geo Energy Geo Resour.* 2025;11(1):12. [[CrossRef](#)].
112. Yang S, Meng D, Yang H, Luo C, Su X. Enhanced soft Monte Carlo simulation coupled with SVR for structural reliability analysis. In: *Proceedings of the Institution of Civil Engineers—Transport.* Leeds, UK: Emerald Publishing Limited; 2025. [[CrossRef](#)].
113. Meng D, Yang H, Yang S, Zhang Y, de Jesus AMP, Correia J, et al. Kriging-assisted hybrid reliability design and optimization of offshore wind turbine support structure based on a portfolio allocation strategy. *Ocean Eng.* 2024;295:116842. [[CrossRef](#)].
114. Kawasaki T, Coslovich D, Ikeda A, Berthier L. Diverging viscosity and soft granular rheology in non-Brownian suspensions. *Phys Rev E Stat Nonlin Soft Matter Phys.* 2015;91(1):012203. [[CrossRef](#)].
115. Johnson LC, Zia RN, Moghimi E, Petekidis G. Influence of structure on the linear response rheology of colloidal gels. *J Rheol.* 2019;63(4):583–608. [[CrossRef](#)].
116. Meng D, Yang S, de Jesus AMP, Fazerer-Ferradosa T, Zhu SP. A novel hybrid adaptive Kriging and water cycle algorithm for reliability-based design and optimization strategy: Application in offshore wind turbine monopile. *Comput Meth Appl Mech Eng.* 2023;412:116083. [[CrossRef](#)].
117. Yang S, Meng D, Wang H, Yang C. A novel learning function for adaptive surrogate-model-based reliability evaluation. *Phil Trans R Soc A.* 2024;382(2264):20220395. [[CrossRef](#)].
118. Meng D, Li Y, He C, Guo J, Lv Z, Wu P. Multidisciplinary design for structural integrity using a collaborative optimization method based on adaptive surrogate modelling. *Mater Des.* 2021;206:109789. [[CrossRef](#)].
119. Meng D, Xie T, Wu P, He C, Hu Z, Lv Z. An uncertainty-based design optimization strategy with random and interval variables for multidisciplinary engineering systems. *Structures.* 2021;32:997–1004. [[CrossRef](#)].
120. Korenaga J. Scaling of stagnant-lid convection with Arrhenius rheology and the effects of mantle melting. *Geophys J Int.* 2009;179(1):154–70. [[CrossRef](#)].
121. Soldati A, Farrell JA, Sant C, Wysocki R, Karson JA. The effect of bubbles on the rheology of basaltic lava flows: Insights from large-scale two-phase experiments. *Earth Planet Sci Lett.* 2020;548:116504. [[CrossRef](#)].
122. Meng D, Wang H, Yang S, Lv Z, Hu Z, Wang Z. Fault analysis of wind power rolling bearing based on EMD feature extraction. *Comput Model Eng Sci.* 2022;130(1):543–58. [[CrossRef](#)].
123. Meng D, Yang S, Lin T, Wang J, Yang H, Lv Z. RBMDO using Gaussian mixture model-based second-order mean-value saddlepoint approximation. *Comput Model Eng Sci.* 2022;132(2):553–68. [[CrossRef](#)].
124. Yang S, Meng D, Wang H, Chen Z, Xu B. A comparative study for adaptive surrogate-model-based reliability evaluation method of automobile components. *Int J Struct Integr.* 2023;14(3):498–519. [[CrossRef](#)].
125. Ma H, Zhu SP, Luo C, Yang S, Meng D. Structural optimization design of metal rubber isolator based on an ensemble surrogate model. *Structures.* 2023;56:104964. [[CrossRef](#)].
126. Yang S, Meng D, Guo Y, Nie P, de Jesus AMP. A reliability-based design and optimization strategy using a novel MPP searching method for maritime engineering structures. *Int J Struct Integr.* 2023;14(5):809–26. [[CrossRef](#)].
127. Ma H, Zhu SP, Guo Y, Pan L, Yang S, Meng D. Residual useful life prediction of the vehicle isolator based on Bayesian inference. *Structures.* 2023;58:105518. [[CrossRef](#)].

128. Murphy E, Lomboy G, Wang K, Sundararajan S, Subramaniam S. The rheology of slurries of athermal cohesive micro-particles immersed in fluid: A computational and experimental comparison. *Chem Eng Sci*. 2019;193:411–20. [[CrossRef](#)].
129. Yang S, He Z, Chai J, Meng D, Macek W, Branco R, et al. A novel hybrid adaptive framework for support vector machine-based reliability analysis: A comparative study. *Structures*. 2023;58:105665. [[CrossRef](#)].
130. Sultangaliyeva F, Carré H, La Borderie C, Zuo W, Keita E, Roussel N. Influence of flexible fibers on the yield stress of fresh cement pastes and mortars. *Cem Concr Res*. 2020;138:106221. [[CrossRef](#)].
131. Guo Y, Meng D, Pan L, Zhang J, Yang S. Reliability evaluation of precision hot extrusion production line based on fuzzy analysis. *Structures*. 2024;64:106553. [[CrossRef](#)].
132. Ley-Hernández AM, Feys D. Effect of sedimentation on the rheological properties of cement pastes. *Mater Struct*. 2021;54(1):47. [[CrossRef](#)].
133. Wang T, Zhang K, Liu Z, Ma T, Luo R, Chen H, et al. Prediction and explanation of debris flow velocity based on multi-strategy fusion Stacking ensemble learning model. *J Hydrol*. 2024;638:131347. [[CrossRef](#)].
134. Coussot P. Yield stress fluid flows: A review of experimental data. *J Non Newton Fluid Mech*. 2014;211:31–49. [[CrossRef](#)].
135. Barnes HA. Rheology of emulsions—A review. *Colloids Surf A Physicochem Eng Asp*. 1994;91:89–95. [[CrossRef](#)].
136. Ruan Y, Liu S, Tang J, Guo Y, Yu T. GLC: A dual-perspective approach for identifying influential nodes in complex networks. *Expert Syst Appl*. 2025;268:126292. [[CrossRef](#)].
137. Denn MM, Bonn D. Issues in the flow of yield-stress liquids. *Rheol Acta*. 2011;50(4):307–15. [[CrossRef](#)].
138. Yang S, De Jesus AMP, Meng D, Nie P, Darabi R, Azinpour E, et al. Very high-cycle fatigue behavior of steel in hydrogen environment: State of the art review and challenges. *Eng Fail Anal*. 2024;166:108898. [[CrossRef](#)].
139. Bran A, Balan C. Fluid rheology prediction using interface detection and machine learning regression. *Phys Fluids*. 2025;37(3):033114. [[CrossRef](#)].
140. Shanahan N, Tran V, Williams A, Zayed A. Effect of SCM combinations on paste rheology and its relationship to particle characteristics of the mixture. *Constr Build Mater*. 2016;123:745–53. [[CrossRef](#)].
141. Meng D, Zhu SP. *Multidisciplinary Design Optimization of Complex Structures Under Uncertainty*. 1st ed. Boca Raton, FL, USA: CRC Press; 2024. [[CrossRef](#)].
142. Brunton SL, Noack BR, Koumoutsakos P. Machine learning for fluid mechanics. *Annu Rev Fluid Mech*. 2020;52:477–508. [[CrossRef](#)].
143. Raissi M, Perdikaris P, Karniadakis GE. Physics-informed neural networks: A deep learning framework for solving forward and inverse problems involving nonlinear partial differential equations. *J Comput Phys*. 2019;378:686–707. [[CrossRef](#)].
144. Ghaboussi J, Pecknold DA, Zhang M, Haj-Ali RM. Autoprogressive training of neural network constitutive models. *Int J Numer Meth Engng*. 1998;42(1):105–26. [[CrossRef](#)].
145. Linka K, Hillgärtner M, Abdolazizi KP, Aydin RC, Itskov M, Cyron CJ. Constitutive artificial neural networks: A fast and general approach to predictive data-driven constitutive modeling by deep learning. *J Comput Phys*. 2021;429:110010. [[CrossRef](#)].
146. Mangal D, Jha A, Dabiri D, Jamali S. Data-driven techniques in rheology: Developments, challenges and perspective. *Curr Opin Colloid Interface Sci*. 2025;75:101873. [[CrossRef](#)].
147. Bahiuddin I, Mazlan SA, Imaduddin F, Shapiai MI, Ubaidillah, Sugeng DA. Review of modeling schemes and machine learning algorithms for fluid rheological behavior analysis. *J Mech Behav Mater*. 2024;33:20220309. [[CrossRef](#)].
148. Brenner MP, Eldredge JD, Freund JB. Perspective on machine learning for advancing fluid mechanics. *Phys Rev Fluids*. 2019;4(10):100501. [[CrossRef](#)].
149. Rackauckas C, Ma Y, Martensen J. Universal differential equations for scientific machine learning. *Proc R Soc A*. 2020;476:20190699. [[CrossRef](#)].
150. Ma T, Shen L, Zhang M, Luo K, Hu X, Jiang Z, et al. Hybrid empirical-data-driven neural network for predicting air-entry value in unsaturated soils. *Math Geosci*. 2025:1–30. [[CrossRef](#)].
151. Ma T, Chen C, Shen L, Luo K, Jiang Z, Liu H, et al. A novel social network search and LightGBM framework for accurate prediction of blast-induced peak particle velocity. *Front Struct Civ Eng*. 2025;19(4):645–62. [[CrossRef](#)].

152. Parolini N, Poiatti A, Vené J, Verani M. Structure-preserving neural networks in data-driven rheological models. *SIAM J Sci Comput.* 2025;47(1):C182–206. [[CrossRef](#)].
153. Mahmoudabadbozchelou M, Caggioni M, Shahsavari S, Hartt WH, Em Karniadakis G, Jamali S. Data-driven physics-informed constitutive metamodeling of complex fluids: A multifidelity neural network (MFNN) framework. *J Rheol.* 2021;65(2):179–98. [[CrossRef](#)].
154. Ma T, Bai P, Zhang H. Multi-objective vehicle delivery path optimization model based on improved constrained evolutionary control operator. In: *2021 2nd International Conference on Artificial Intelligence and Information Systems*; 2021 May 21–30; Chongqing China. p. 1–5. [[CrossRef](#)].
155. Ma T, Lin Y, Zhou X, Zhang M. Grading evaluation of goaf stability based on entropy and normal cloud model. *Adv Civ Eng.* 2022;2022(1):9600909. [[CrossRef](#)].
156. El Moçayd N, Seaid M. Data-driven polynomial chaos expansions for characterization of complex fluid rheology: Case study of phosphate slurry. *Reliab Eng Syst Saf.* 2021;216:107923. [[CrossRef](#)].
157. Ma T, Chen C, Shen L, Luo K, Jiang Z, Xie S, et al. Physics-informed neural networks for capturing the true relationships between parameters to predict the dynamic triaxial strength of rocks in cold environments. *Measurement.* 2026;257:118900. [[CrossRef](#)].
158. Nazar S, Yang J, Iqbal M, Xie J, Farooq F. Computational intelligence for modeling the rheological properties of the developed hydrated lime-based alkali-activated materials. *Mater Today Commun.* 2024;41:110602. [[CrossRef](#)].
159. Noack BR, Morzyński M, Tadmor G. *Reduced-Order Modelling for Flow Control*. Berlin/Heidelberg, Germany: Springer; 2011 [[CrossRef](#)].
160. Luo K, Peng K, Ma T, Luo S, Liu X, Wu T, et al. Understanding the combined effect of dynamic impact and water saturation on dynamic tensile behavior of sandstone. *Eng Fract Mech.* 2026;335:111918. [[CrossRef](#)].